HHS Public Access

Author manuscript

Clin Cancer Res. Author manuscript; available in PMC 2018 November 15.

Published in final edited form as:

Clin Cancer Res. 2017 November 15; 23(22): 6958–6968. doi:10.1158/1078-0432.CCR-17-0803.

Combined CDK4/6 mTOR inhibition is synergistic against glioblastoma via multiple mechanisms

Inan Olmez[1], **Breanna Brenneman**[1], **Aizhen Xiao**[1], **Vlad Serbulea**[2], **Mouadh Benamar**[3], **Ying Zhang**[4], **Laryssa Manigat**[1], **Tarek Abbas**[3], **Jeongwu Lee**[5], **Ichiro Nakano**[6], **Jakub Godlewski**[7], **Agnieszka Bronisz**[7], **Roger Abounader**[4], **Norbert Leitinger**[2], and **Benjamin Purow**[1,*]

[1]Department of Neurology, University of Virginia, Charlottesville, VA 22908, USA

[2]Department of Pharmacology, University of Virginia, Charlottesville, VA 22908, USA

[3]Department of Radiation Oncology, Biochemistry, and Molecular Genetics, University of Virginia, Charlottesville, VA 22908, USA

[4]Department of Microbiology, Immunology, and Cancer Biology, University of Virginia, Charlottesville, VA 22908, USA

[5]Department of Stem Cell Biology and Regenerative Medicine, Lerner Research Institute, Cleveland Clinic, Cleveland, OH 44195, USA

[6]Department of Neurosurgery, University of Alabama, Birmingham, AL 35233, USA

[7]Department of Neurosurgery, Brigham and Women's Hospital, Boston, MA 02115, USA

Abstract

Purpose—Glioblastoma (GBM) is a deadly brain tumor marked by dysregulated signaling and aberrant cell cycle control. Molecular analyses have identified that the CDK4/6-Rb-E2F axis is dysregulated in about 80% of GBMs. Single-agent CDK4/6 inhibitors have failed to provide durable responses in GBM, suggesting a need to combine them with other agents. We investigate the efficacy of the combination of CDK4/6 inhibition and mTOR inhibition against GBM.

Experimental Design—Preclinical *in vitro* and *in vivo* assays using primary GBM cell lines were performed.

Results—We show that the CDK4/6 inhibitor palbociclib suppresses the activity of downstream mediators of the mTOR pathway, leading to rebound mTOR activation that can be blocked by the mTOR inhibitor everolimus. We further show that mTOR inhibition with everolimus leads to activation of the Ras mediator Erk that is reversible with palbociclib. The combined treatment strongly disrupts GBM metabolism, resulting in significant apoptosis. Further increasing the utility of the combination for brain cancers, everolimus significantly increases the brain concentration of palbociclib.

[*]Corresponding Author: Benjamin Purow, M.D., University of Virginia, Old Medical School, Room 4881, 21 Hospital Drive, Charlottesville, VA 22908, USA. Phone: 434-924-5545, Fax: 434-982-4467, bwp5g@virginia.edu.

Conclusions—Our findings demonstrate that the combination of CDK4/6 and mTOR inhibition has therapeutic potential against GBM and suggest it should be evaluated in a clinical trial.

Keywords

CDK4/6; mTOR; Glioblastoma; palbociclib; everolimus

INTRODUCTION

Glioblastoma (GBM) is the most common primary brain tumor, with an extremely poor prognosis (1). The efficacy of standard therapy is limited, providing only 15–18 months of median survival from the initial diagnosis (2), and clinical trials have largely proven disappointing. The resistance of GBM to standard therapies seems to be multifactorial. With recent advances, it is now known that GBMs harbor a small subpopulation of treatment-resistant glioma-initiating cells (GICs) that may drive recurrence (3). Thus, developing new therapies using GICs may improve the devastating prognosis of GBM. GBM is also marked by genetic heterogeneity and adaptability that likely contribute to the resistance to single therapies; identifying rational and effective combination therapies is therefore more likely to have an impact.

The CDK4/6-Rb-E2F axis controls the cell cycle and is tightly regulated by several factors such as cyclin-D, INK4 family proteins ($p15^{INK4b,}$ $p16^{INK4a}$, $p18^{INK4c}$, and $p19^{INK4d}$), $p21^{CIP1}$, and $p27^{KIP1}$. One of the hallmarks of GBM is aberrant cell cycle control, resulting in unlimited cell cycle re-entry and progression. According to The Cancer Genome Atlas (TCGA) database, homozygous deletion of the *p16INK4a* gene occurs in 50% of GBMs. Other common cell cycle-related mutations in GBM include amplification and over-expression of *CDK4* and homozygous deletion/mutation of *RB*, followed in frequency by over-expression of cyclin D1 and amplification of *CDK6* (4,5). Overall, the CDK4/6-Rb-E2F axis is deregulated in about 80% of GBMs, underscoring the importance of targeting the cell cycle in GBM.

Palbociclib (PD0332991), a specific CDK4/6 inhibitor, was developed to arrest cell cycle progression in proliferating tumor cells. It proved to be beneficial especially in tumors lacking p16INK4a or over-expressing cyclin D such as bladder and gastric cancers, while those without functional *RB1* have been refractory to palbociclib treatment. Upon promising results in preclinical models of various cancers including GBM (6,7), palbociclib has been tested in several phase I/II clinical trials and has been approved by the FDA in combination with anti-estrogen therapies against hormone receptor-positive breast cancers (8,9). These clinical studies indicate that palbociclib as a single agent fails to provide durable responses, potentially due at least in part to tumor adaptation, and suggesting a need to combine with other agents. While modifications in several cell cycle regulators such as activation of CDK2, amplification of cyclin D, and loss of $p21^{CIP1}$ or $p27^{KIP1}$ may contribute to tumor adaptation, the main resistance to palbociclib treatment is mediated by *RB1* inactivation (10–12). We therefore sought a combination regimen using palbociclib that inhibits overall cell cycle progression.

We performed enrichment analysis through the online Cancer Therapeutics Response Portal (CTRP) and found that mutations in *RB1* and *CCND3* increased sensitivity to an mTOR inhibitor, sirolimus. This finding is supported by studies showing inverse correlations between the RB pathway and mTOR activity (13,14). Despite initial promising results, single-agent mTOR inhibitors failed to achieve durable therapeutic responses against GBM due to several reasons including their cytostatic nature, modest brain penetration, and importantly the reactivation of Akt (15). Therefore, with this study we assessed for the first time the efficacy of the combination of CDK4/6 and mTOR inhibition against GBM. We show both *in vitro* and *in vivo* that palbociclib synergizes with the mTOR inhibitor everolimus through several distinct mechanisms.

MATERIALS AND METHODS

Cell culture, drug sensitivity, and self-renewal assays

Human primary GIC lines were received from Jeongwu Lee (Cleveland Clinic) and Jakub Godlewski (Brigham and Women's Hospital) in 2014. All cell lines were verified as human cells with short tandem repeat profiling before and during the experimental procedures. At the beginning of *in vitro* experiments, all cell lines tested negative for mycoplasma contamination by PCR and repeat testing was done every four weeks. Cell lines were further validated by gene expression analysis for stem cell markers (SOX2, CD133, OLIG2, and CD44) and self-renewal assay. New cells were thawed every four weeks and the passage number of each line was <10 throughout the study. GIC lines were cultured as neurospheres using neurobasal media supplemented with N2 (ThermoFisher), B27 (ThermoFisher), EGF (20 ng/ml, R&D), and FGF (20 ng/ml, R&D). All *in vitro* assays were performed in adherent conditions using laminin (Corning) coated plates. Ethylenediaminetetraacetic acid (EDTA) 0.02% (Lonza) was used to split spheres into individual cells. Cell viability was measured three days after drug treatments with both TrypanBlue exclusion/cell counting using Cellometer Auto T4 (Nexcelom) and alamarBlue (ThermoFisher Scientific). Ribociclib (S7440), palbociclib (S1116) and everolimus (S1120) were purchased from Selleckchem. Temsirolimus (5264) was from Tocris. Self-renewal assays were performed with ultra-low attachment plates (Corning) and interpreted as described previously (16).

Animal studies

All mouse studies were approved by the Institutional Animal Care and Use Committee (IACUC) at the University of Virginia. 5,000 G2 or 400,000 G528 GICs were stereotactically injected into the right striatum of six-to-eight-week-old female BALB/c SCID NCr mice. Mice were then randomized into 4 groups: control, palbociclib only, everolimus only, and the combination of both. 100 μl of palbociclib (10 mg/ml in water) or everolimus (1 mg/ml in water) were given once-daily for four days a week via oral gavage. Mice were euthanized when they showed neurological symptoms or were at a moribund stage. Mouse survival was compared between groups. The sample size for each group was established based on our experience using the predicted calculation (median survival for control group would be 35 days, treatment group would be 130 days, maximum follow-up would be 250 days with power of 85%). No animals were excluded from the outcome analysis.

Immunoblotting, antibody array (ELISA), and Caspase-3/7 assay

Immunoblotting was performed as previously described (17). The following antibodies were used for immunoblotting: Bcl-2 (sc-7382), Cyclin A (sc-751), CDK4 (sc-260), CDK6 (sc-177), and mTOR (sc-1549) antibodies were from Santa Cruz, Actin (A5441) and GAPDH (G9545) were from Sigma-Aldrich, and all other antibodies including Cyclin D1 (2978), PARP (9542), phospho-mTOR^{Ser2448} (2971), phospho-p70 S6K^{Thr389} (9234), phospho-S6$^{Ser235/236}$ (4858), p70 S6K (2708), S6 (2317), phospho-p44/42 Erk1/2$^{Thr202/Tyr204}$ (9101), and p44/42 Erk1/2 (9102) as well as antibody array kit (7949) were from Cell Signaling. The antibody array was performed according to the manufacturer's instructions and slides were scanned with a fluorescent reader. The Caspase-Glo 3/7 Assay kit (G8090, Promega) was used for detecting Caspase 3/7 levels according to the manufacturer's instructions following 2 days of drug treatment.

Plasmid and siRNA transfection

Constitutively-active CDK4 (RC401060, Origene) and mTOR (69010, Addgene) as well as the respective control plasmids were used for rescue experiments. 125,000 cells were seeded into a laminin-coated 12-well plate and the next day plasmid transfection was performed using Fugene HD (Promega) according to the manufacturer's instructions. 24 hours after the transfection, treatment with the combination of palbociclib and everolimus was started and cell counts were compared following 2 days of treatment. Lipofectamine® RNAiMAX (13778150, ThermoFisher Scientific) was used for siRNA transfection according to the manufacturer's instructions with final siRNA concentration of 10 nmol/L. All siRNAs including control, CDK4, CDK6, and mTOR siRNAs are from Dharmacon SMARTpool ON-TARGETplus.

Flow cytometry

The effects of drug treatments on cell cycle distribution of proliferating GICs were assessed with propidium iodide staining using flow cytometry. Asynchronous GICs were treated with palbociclib, everolimus, or the combination for 24 hours. Each condition was done in triplicate. Cells were washed with 1X PBS, harvested using Trypsin, washed a second time with 1X PBS, and then fixed in 1mL of 75% Ethanol. Cells were treated with 1X PI staining buffer (containing 50ug/mL propidium iodide, 10ug/mL RNAse and 0.05% NP40). Samples were acquired using a BD FACSCalibur and cell cycle distribution was analyzed using FlowJo and Modfit softwares.

Immunohistochemistry staining

Immunohistochemistry was performed on a robotic platform (Ventana discover Ultra Staining Module, Ventana Co., Tucson, AZ, USA). Tissue sections (4 μm) were first fixed with acetone:methanol (1:1 ratio) for 10 minutes. Endogenous peroxidases were blocked with peroxidase inhibitor (CM1) for 8 min before incubating the section with either antibody to Nestin (Sigma Prestige, Cat#HPA 007007) or CD133 (Abcam, Cat#ab19898) both at 1:100 dilution for 60 min at room temperature. Antigen-antibody complex was then detected using DISCOVERY OmniMap Anti-Rb HRP detection system and DISCOVERY

ChromoMap DAB Kit (Ventana Co.). All the slides were counterstained with hematoxylin subsequently; they were dehydrated, cleared and mounted for the assessment.

Glycolytic and Mitochondrial Stress Tests

Cells were seeded as a monolayer into a laminin-coated Seahorse 24-well tissue culture plate (Agilent Technologies, Santa Clara, CA). For assessing respiratory capacity, cells were subjected to a mitochondrial stress test following 48h of drug treatments. At the beginning of the assay, the media was changed to DMEM with pyruvate and cells were allowed to equilibrate for 30 minutes at 37°C. Oxygen consumption rate (OCR) was measured using a Seahorse XF24 Flux Analyzer (Agilent Technologies, Santa Clara, CA). After three basal OCR measurements, OCR for the treatment plates was measured using four-minute measurement periods. Compounds to modulate cellular respiratory function [1μM Oligomycin (Sigma-Aldrich); 2μM BAM15 (Cayman Chemical Company); 1μM Antimycin A & 100nM Rotenone (Sigma-Aldrich)] were injected after every three measurements. Basal respiration was calculated by subtracting the average of the first three measurements by the average of the post-Antimycin A & Rotenone measurements. Maximum respiratory capacity was calculated by subtracting the average of the post-BAM15 measurements by the average of the post- Antimycin A & Rotenone measurements. The reserve capacity was calculated by subtracting the average of the basal measurements from the average of the post-BAM15 measurements.

For assessing glycolytic capacity, cells were subjected to a glycolytic stress test following 48h of drug treatments. For this test, extracellular acidification rate (ECAR), representing the secretion of lactate, was measured using a Seahorse XF24 Flux Analyzer. At the beginning of the assay, the media was changed to unbuffered, glucose-free, DMEM (Sigma-Aldrich Cat#:D5030, pH=7.35 at 37°C), supplemented with 143mM NaCl and 2mM Glutamine. After three basal ECAR measurements, ECAR for the treatment plates was measured using three-minute measurement periods. Compounds to modulate glycolysis (20mM Glucose; 1μM Oligomycin; 80mM 2-Deoxyglucose) (Sigma) were injected after every three measurements. Basal glycolysis was calculated by subtracting the average of the post- 2-Deoxyglucose measurements from the average of the post-Glucose measurements. Maximum glycolytic capacity was calculated by subtracting the average of the post- 2-Deoxyglucose measurements from the average of the post-Oligomycin measurements. The glycolytic reserve capacity was calculated by subtracting the average of the post-Oligomycin measurements from the average of the post-Glucose measurements.

In vitro cellular palbociclib accumulation analysis

150,000 hCMEC/D3 cells were seeded into a collagen coated 12-well plate and allowed to attach to the plate overnight. The next day, cells were treated with everolimus or elacridar during the preincubation phase (30 minutes), followed by the addition of palbociclib for 1 hour (accumulation phase). After the accumulation phase, cells were washed with PBS two times and lysed by sonication. Samples were kept at −80 °C overnight and intracellular palbociclib concentration was measured by the LC-MS system.

Detection of palbociclib in mouse plasma and brain homogenate samples by LC/MS-MS

Mice were randomized into two groups: palbociclib only and the combination of palbociclib and everolimus. Mice were treated with 100 μl of palbociclib (10 mg/ml in water) and/or everolimus (1 mg/ml in water) once-daily for three days. Both blood and brain samples were collected 6 hours after the third dose. Brain samples were weighed and homogenized in 4 volumes of water with a tissue homogenizer (VWR, 47747-370). Acetonitrile was used as precipitant. Two separate standard curves were set up for detecting palbociclib from blood and brain samples. The samples were injected as supplied in 90% acetonitrile (10uL). The LC-MS system consisted of a Thermo Electron TSQ Quantum Access MAX mass spectrometer system with a HESI source interfaced to an Agilent ZORBAX Eclipse XDB 80Å C18, 4.6 × 150 mm, 5 μm HPLC column (Part number: 993967-902) reversed-phased column. 10 uL was injected and the compounds eluted from the column by an acetonitrile/ 0.1% formic acid with 10 mM ammonium acetate gradient at a flow rate of 500 μL/min over 23 min. The nanospray ion source was operated at +2.6 kV. The following multiple reaction monitoring (MRM) was used for Palbociclib (448.0 – 380.0). The data was analyzed using the peak area (MRM) in each sample and comparing it to areas obtained for standard curve generated at the start of the sample set. Sufficient blanks were run between samples to ensure no signal for any compound was detected before proceeding in the set.

Statistics and synergy calculations

We utilized two different synergy calculation methods: the Bliss difference and the Chou-Talalay (ComboSyn). With the Chou-Talalay method, combination indices (CI) were generated and CI less than 1 was considered to be synergistic, whereas less than 0.2 was considered strong synergy (18). The Bliss method was also used for synergy calculation as described previously (19). The Bliss value is the difference between active and predicted cytotoxicity of a combination therapy. When the Bliss difference is zero, two agents are considered to be additive, whereas greater than zero indicates synergy and less than zero indicates antagonism. This method is useful even when one of the components of a combined treatment fails to provide notable response.

GraphPad Prism 6 (GraphPad Software) was used for general statistical analyses. For 2-group comparisons, Student’s t-test and for multiple group comparisons, one-way ANOVA with post-hoc Tukey analysis were utilized. P-values less than 0.05 were considered significant using an error rate α=0.05. Mouse survival curve was generated with Kaplan-Meier analysis. Sample sizes were chosen based on our prior experience and power calculation of 85%.

RESULTS

Combining CDK4/6 and mTOR inhibitors exhibits synergy *in vitro* against GICs and induces apoptosis

The mTOR inhibitor everolimus modifies various important cellular functions including the cell cycle. With the Cancer Therapeutics Response Portal, an online resource from the Broad Institute describing the responses of 860 well-characterized cancer lines to 481 agents (http://portals.broadinstitute.org/ctrp/), we found that mutations in both *RB1* and *CCND3*

increased sensitivity to the mTOR inhibitor sirolimus (Fig. 1A and Supplementary Fig. S1). Since *RB1* mutation is a cancer resistance mechanism for CDK4/6 inhibitors, we hypothesized that mTOR inhibition might help block this pathway to overcome the resistance. We therefore assessed the efficacy of palbociclib and everolimus on established patient-derived GIC lines *in vitro* in combination and singly. Given the potential for *RB1* mutations to affect the response to CDK4/6 inhibitors, we sequenced the *RB1* gene in our cell lines and detected only a silent mutation within exon 10 in one of them (G528); there was no alteration in Rb1 amino acid sequence in any line. Both drugs reduced cell viability in a dose-dependent manner (Supplementary Fig. S2). Using two different statistical methods, we then showed significant synergy between palbociclib and everolimus even at low concentrations (Fig. 1B). Since neurosphere formation *in vitro* is correlated with tumor-forming potential of GICs (17), we tested with a self-renewal assay and observed that the combined treatment suppressed sphere formation significantly (Fig. 1C). We further confirmed synergistic interaction by using different mTOR and CDK4/6 inhibitors (Fig. 1D). To exclude potential off-target effects from specific inhibitors, we also showed synergy when replacing either inhibitor with the relevant siRNAs (Fig. 1E). To further support that the inhibitions of CDK4/6 and mTOR are the main mechanistic drivers of the toxicity of the combination treatment, we demonstrated that constitutively-active CDK4 and mTOR plasmids were able to partially rescue from the combination treatment-induced cell death (Fig. 1F). Having demonstrated significant synergy with the combination therapy, we initially looked for effects of the combination on the cell cycle; we noted that enhanced synergy may be due in part to more efficient suppression of the cell cycle with the combined therapy (Supplementary Fig. S3).

Both palbociclib and everolimus are generally considered cytostatic agents that inhibit cell growth and proliferation; compared to cytotoxic agents, they induce minimal apoptosis—especially palbociclib (20). Having observed a significant reduction in cell viability, we questioned whether the combined treatment triggered cell death through induction of apoptosis. We demonstrated with immunoblot and a caspase-3/7 assay that the combination of palbociclib and everolimus induced notable apoptosis, while apoptosis was minimal with individual treatments (Fig. 1G and 1H).

Palbociclib and everolimus cooperate through multiple signaling pathways

Several studies have reported that inactivation of the RB pathway leads to over-expression of mTOR (13,14), and palbociclib is known to drive *RB1* inactivation as a resistance mechanism (10,11). We therefore assessed the activation status of mTOR in GIC lines upon palbociclib exposure. Palbociclib treatment led to higher mTOR activity, which was completely reversed by the combined treatment (Fig. 2A). Although palbociclib can ultimately cause *RB1* inactivation, this no doubt requires a longer duration of palbociclib therapy.

In addition to direct regulation of each other, we also considered effects on downstream mediators. Studies have shown multiple points of crosstalk between the oncogenic Akt/mTOR and Ras/Erk pathways, including elevation of MAPK activity by mTOR inhibition (21,22). Based on this, we assessed the effects of the compounds singly and in combination

on Erk activation. We were surprised to note that palbociclib treatment suppressed Erk activity (Fig. 2A), which could in part explain a compensatory activation of mTOR. We further demonstrated with *CDK4/6*-specific siRNAs that suppression of Erk activity is indeed linked to CDK4/6 inhibition or knockdown rather than being an off-target effect from palbociclib (Supplementary Fig. S4). As expected, everolimus treatment elevated Erk activity, which was significantly reversed by addition of palbociclib (Fig. 2A).

In a recent study on lung cancer, palbociclib was shown to interact with several protein and lipid kinases beyond CDK4/6 (23). Based on this report and our unexpected finding in Figure 2A, we performed screening for other potential targets with a commercial antibody array kit. Notably, phosphorylation of S6 was significantly reduced upon 48h of palbociclib treatment (Fig. 2B). We subsequently confirmed this with immunoblot (Fig. 2C). While the antibody array also showed suppressed Erk activity, there was not any significant change in Akt activity with palbociclib treatment (Supplementary Fig. S5). The ribosomal protein S6 is one of the main downstream mediators of the mTOR pathway. It has significant roles in protein synthesis, cell cycle progression, and energy metabolism. Its activity is regulated by p70S6 kinase (p70S6K) through phosphorylation, suggesting that palbociclib might be decreasing phosphorylation of S6 through suppression of p70S6K activity. We confirmed with immunoblot that palbociclib indeed decreased the activity of p70S6K (Fig. 2D).

Combined CDK4/6 and mTOR inhibition disrupts GIC metabolism

The mTOR pathway is an important signaling node that regulates various critical cellular functions such as metabolism, cell survival, protein synthesis, and cell cycle progression. When activated, mTOR induces metabolic rearrangements in the form of increased glycolysis and mitochondrial metabolism accompanying protein and lipid biosynthesis and cell growth (24). Given the mTOR effects on metabolism and the above-noted crosstalk between CDK4/6 inhibition and mTOR inhibition, we assessed the effects of CDK4/6 inhibition and combined CDK4/6/mTOR inhibition on GIC metabolism. We initially evaluated oxygen consumption as a measure of oxidative phosphorylation. We observed that similarly to everolimus, palbociclib inhibited the maximum respiratory capacity in GIC lines. More importantly, the combination of palbociclib and everolimus showed a synergistic effect, completely abolishing oxidative mitochondrial function even at a low dose and duration that did not induce substantial cytotoxicity (Fig. 3A). We next evaluated the media acidification rate with the glycolytic stress test, an indicator of lactate production. This alternative pathway for the glucose-derived metabolite, pyruvate, leads to moderate but inefficient ATP production, and is a hallmark of cancer cells known as the Warburg effect (25). Our results indicated that both everolimus and pablociclib inhibited aerobic glycolysis. Furthermore, this effect was more pronounced when both drugs were combined (Fig. 3B). Since excessive cell detachment can produce similar results, we confirmed that nearly all the cells were still attached after the washing process and at the end of the run (Supplementary Fig. S6). Taken together, these data have significant implications; similar to everolimus, palbociclib also inhibits glucose metabolism in GICs, and palbociclib-induced metabolic rearrangement may in part be responsible for rebound mTOR activation. Additionally, the dramatic metabolic inhibitory effects observed with the combined treatment likely contribute to cell death, potentially explaining the significant apoptosis demonstrated earlier.

Everolimus significantly increases the brain concentration of palbociclib

Despite technological advances, efficient drug delivery across the blood-brain barrier (BBB) remains a major obstacle in the treatment of GBM, limiting therapeutic options. In addition to the physical barrier, the BBB harbors multidrug ATP binding cassette (ABC) transporters such as P-glycoprotein (P-gp, ABCB1) and breast cancer resistance protein (BCRP1, ABCG2), further restricting brain delivery of therapeutic agents (26,27). Given the significance of the BBB, the success of a combination therapy in part hinges on the level of brain distribution and achieving therapeutically relevant concentrations. One approach consists of designing combination therapies with two active agents in which one agent inhibits the BBB efflux transporters lowering concentrations of the other agent. In a recent study, everolimus was shown to be a potent inhibitor of both P-gp and BCRP1 *in vitro*. Based on this, when combined with vandetanib, everolimus was shown to increase both cellular accumulation and brain penetration of vandetanib (26). Like many other anti-tumor agents, palbociclib is also subject to efflux by BBB transporters. Recent *in vivo* studies showed that both P-gp and BCRP restricted brain penetration of palbociclib, resulting in low drug levels (28,29). Therefore, we compared brain concentrations in mice of palbociclib when used alone vs. in combination with everolimus. All mice were treated with once-daily oral palbociclib (50 mg/kg/day) for three days. We showed that concurrent treatment of palbociclib and once-daily oral everolimus (5 mg/kg/day) for three days significantly increased both brain concentration and brain-blood ratio of palbociclib about two-fold (Fig. 4A and 4B). We further tested our hypothesis that everolimus affects palbociclib retention in the brain using an *in vitro* BBB-relevant system with an immortalized human brain endothelial cell line (hCMEC/D3). We showed that everolimus increases cellular accumulation of palbociclib in a dose-dependent manner (Fig. 4C). We also tested elacridar, a very potent inhibitor of P-gp and BCRP, and found a roughly two-fold increase in intracellular palbociclib concentration (Fig. 4D). Our findings suggest that everolimus promotes palbociclib retention in the BBB and brain and that it may be combined with other drugs to increase their brain concentration. These results provided a further rationale for testing this combination *in vivo* against GBM.

Combinatorial efficacy of CDK4/6 and mTOR inhibition against aggressive orthotopic GIC models *in vivo*

Our *in vitro* findings prompted us to evaluate the efficacy of the palbociclib and everolimus combination in orthotopic GBM models using three GIC lines. Mice were treated with vehicle, once-daily oral palbociclib (50 mg/kg/day, four days a week), once-daily oral everolimus (5 mg/kg/day, four days a week), or the combination of palbociclib and everolimus. While these doses of each individual drug failed to yield significant therapeutic responses, the combined treatment prolonged median and overall survival significantly in both GIC lines tested (Fig. 5A–B). We also assessed expression of GIC markers including nestin and CD133 in tumor-harboring mouse brains from control vs. the combination group, and there was a clear decrease in tumor expression of these markers with the combination treatment (Supplementary Fig. S7). We did not observe major toxicity from the individual or combined drug treatments, as indicated by comparable mouse weights and no signs of ill health in all treatment groups (Fig. 5C). We recapitulated some of our *in vitro* findings with immunoblot using mouse brain samples (Fig. 5D). Overall, we have shown both *in vitro* and

in vivo that palbociclib and everolimus cooperate through several mechanisms, and that the combination of both exhibits significant synergy against GICs. A schematic summarizing the identified CDK4/6/mTOR interactions is shown in Figure 6.

DISCUSSION

The clinical efficacy of single-agent CDK4/6 and mTOR inhibitors against GBM and other cancers has been limited by a number of factors. These have included the cytostatic nature of both agents, the emergence of *RB1*-mutated resistant clones for CDK4/6 inhibitors, and feedback elevation of Akt activity for mTOR inhibitors. Single-agent palbociclib has failed to provide durable therapeutic response in various clinical trials (8,30), prompting a search for combinatorial approaches. The greatest success has emerged in combining CDK4/6 inhibitors with anti-estrogenic therapies in hormone-positive breast cancers (9). Given the regulatory role of the Ras pathway on the cell cycle, palbociclib has been studied in combination with MEK inhibitors against Ras-mutated tumors such as melanoma and pancreatic cancer (12,31). An early report of a phase I/II trial combining another CDK4/6 inhibitor, LEE011, and binimetinib (MEK162) highlighted promising results against Ras-mutated melanoma (32). Despite significant drug-related toxicities, this fueled further clinical trials combining palbociclib with different MEK inhibitors (NCT02022982, NCT02065063). At this stage it is unclear whether this combination strategy will hold promise against cancers such as GBM with relatively lower frequencies of Ras mutations.

Unlike palbociclib, single-agent everolimus has proven successful against certain tumors, including pancreatic neuroendocrine tumors, carcinoid tumors of the lung and gastrointestinal tract, advanced renal cell carcinoma, and subependymal giant cell astrocytoma (SEGA) associated with tuberous sclerosis (33–36). Results of clinical trials in GBM using everolimus as a single agent or in combination have been disappointing (15,37). Our findings have shown that combining CDK4/6 and mTOR inhibitors offers increased benefits against GBM through a number of mechanisms—including blockade of compensatory signaling mechanisms, improved brain penetration of palbociclib, enhanced metabolic effects, and cytostatic to cytotoxic conversion. A few recent reports have identified benefit in combining CDK4/6 and Akt or mTOR inhibition in other cancers (38,39), but these have been in different contexts and did not identify the biologic rationales noted here.

The BBB continues to constitute a major obstacle for GBM treatment. Given the fact that most chemotherapeutics are subject to efflux by active transporters within the BBB, the recent finding that everolimus blocks the activity of these transporters may contribute to new combination strategies to improve delivery as well as complement each other's direct anti-cancer activity (26). Following up on the everolimus BBB finding, a group at MD Anderson successfully combined everolimus with vandetanib as a strategy to enhance the brain concentration of vandetanib against lung cancer metastatic to brain (40). Similarly, we showed that when combined with everolimus, palbociclib had almost 2-fold higher brain concentration. This may have clinical implications; besides potentially increased efficacy due to better brain penetration, palbociclib dose reduction could be considered to minimize toxicity. Palbociclib toxicities including thrombocytopenia, neutropenia, anemia, and fatigue

have been reported in various clinical trials (41,42). These adverse effects may potentially be more pronounced with the combined treatment, possibly worsening quality-of-life. Thus, dose reduction with the combined treatment may help patients maintain quality-of-life without losing efficacy against the tumor.

Aberrant cancer metabolism has increasingly been recognized as a potential therapeutic target (43,44). It is now known that many anti-cancer agents, including palbociclib and everolimus, induce metabolic changes that can render cancer cells more sensitive to specific targeted agents and chemotherapeutics. In general, the cell cycle is coupled to cellular metabolism such that the cell cycle becomes active or inactive during high or low levels of cellular metabolism, respectively. This is due at least in part to shared control by upstream regulators such as CDK4 and cyclin D1. For instance, CDK4 and cyclin D1 expression or Rb inactivation have been shown to increase cellular metabolism while inducing proliferation (45–47). As might have been expected, we showed that palbociclib inhibits cellular metabolism similarly to everolimus, and the combination of both drugs potentiates this metabolic effect. Interestingly, we have shown that in addition to cell cycle inhibition, palbociclib also suppresses the activity of mTOR's downstream mediators, p70S6K and S6, likely potentiating the metabolic effects. In line with previous studies (38), we demonstrated that palbociclib activates mTOR—which is likely due to feedback mechanisms from suppression of mTOR downstream mediators, of cellular metabolism, and of the cell cycle. Contrasting with our results, a recent report on palbociclib-induced metabolic reprogramming in Ras-mutated pancreatic cancer (38) showed that palbociclib treatment activated both glycolytic and mitochondrial metabolism through mTOR activation. These differences could be due to the presence of Ras mutation in the pancreatic cancer model or to the different tissue contexts.

Clinical trials have shown that in general, single-agent treatments provide limited benefits—due at least in part to tumor adaptation. Thus, combination therapies have typically been more successful in cancer therapy. One key strategy for designing drug combinations is to provide maximal efficacy through synergistic drug-drug interaction while using minimal doses to reduce adverse effects. Our results suggest that combining CDK4/6 and mTOR inhibition may be a good fit for this strategy in GBM indicating a need to evaluate this in a clinical trial.

Supplementary Material

Refer to Web version on PubMed Central for supplementary material.

Acknowledgments

Financial support: National Institutes of Health (NIH) grants 5R01CA180699, 1R01CA189524 (B.P.), R01 DK096076, and P01 HL120840 (N.L.).

We would like to thank Drs. Sherman and Park at the W.M. Keck Biomedical Mass Spectrometry Laboratory, funded by a grant from the University of Virginia's School of Medicine. V.S. is a recipient of T32 Training Grant: T32 GM007055-42, AHA Fellowship: 15PRE25560036, and NIH F31 Fellowship: F31 DK108553-01A1.

References

1. Hess KR, Broglio KR, Bondy ML. Adult glioma incidence trends in the United States, 1977–2000. Cancer. 2004; 101(10):2293–9. DOI: 10.1002/cncr.20621 [PubMed: 15476282]
2. Stupp R, Mason WP, van den Bent MJ, Weller M, Fisher B, Taphoorn MJ, et al. Radiotherapy plus concomitant and adjuvant temozolomide for glioblastoma. N Engl J Med. 2005; 352(10):987–96. DOI: 10.1056/NEJMoa043330 [PubMed: 15758009]
3. Singh SK, Hawkins C, Clarke ID, Squire JA, Bayani J, Hide T, et al. Identification of human brain tumour initiating cells. Nature. 2004; 432(7015):396–401. DOI: 10.1038/nature03128 [PubMed: 15549107]
4. CancerGenomeAtlasResearchNetwork. Comprehensive genomic characterization defines human glioblastoma genes and core pathways. Nature. 2008; 455(7216):1061–8. nature07385 [pii]. DOI: 10.1038/nature07385 [PubMed: 18772890]
5. Parsons DW, Jones S, Zhang X, Lin JC, Leary RJ, Angenendt P, et al. An integrated genomic analysis of human glioblastoma multiforme. Science. 2008; 321(5897):1807–12. DOI: 10.1126/science.1164382 [PubMed: 18772396]
6. Barton KL, Misuraca K, Cordero F, Dobrikova E, Min HD, Gromeier M, et al. PD-0332991, a CDK4/6 inhibitor, significantly prolongs survival in a genetically engineered mouse model of brainstem glioma. PLoS One. 2013; 8(10):e77639.doi: 10.1371/journal.pone.0077639 [PubMed: 24098593]
7. Michaud K, Solomon DA, Oermann E, Kim JS, Zhong WZ, Prados MD, et al. Pharmacologic inhibition of cyclin-dependent kinases 4 and 6 arrests the growth of glioblastoma multiforme intracranial xenografts. Cancer Res. 2010; 70(8):3228–38. DOI: 10.1158/0008-5472.CAN-09-4559 [PubMed: 20354191]
8. Asghar U, Witkiewicz AK, Turner NC, Knudsen ES. The history and future of targeting cyclin-dependent kinases in cancer therapy. Nat Rev Drug Discov. 2015; 14(2):130–46. DOI: 10.1038/nrd4504 [PubMed: 25633797]
9. Walker AJ, Wedam S, Amiri-Kordestani L, Bloomquist E, Tang S, Sridhara R, et al. FDA Approval of Palbociclib in Combination with Fulvestrant for the Treatment of Hormone Receptor-Positive, HER2-Negative Metastatic Breast Cancer. Clin Cancer Res. 2016; 22(20):4968–72. DOI: 10.1158/1078-0432.CCR-16-0493 [PubMed: 27407089]
10. Wiedemeyer WR, Dunn IF, Quayle SN, Zhang J, Chheda MG, Dunn GP, et al. Pattern of retinoblastoma pathway inactivation dictates response to CDK4/6 inhibition in GBM. Proc Natl Acad Sci U S A. 2010; 107(25):11501–6. DOI: 10.1073/pnas.1001613107 [PubMed: 20534551]
11. Dean JL, Thangavel C, McClendon AK, Reed CA, Knudsen ES. Therapeutic CDK4/6 inhibition in breast cancer: key mechanisms of response and failure. Oncogene. 2010; 29(28):4018–32. DOI: 10.1038/onc.2010.154 [PubMed: 20473330]
12. Franco J, Witkiewicz AK, Knudsen ES. CDK4/6 inhibitors have potent activity in combination with pathway selective therapeutic agents in models of pancreatic cancer. Oncotarget. 2014; 5(15):6512–25. DOI: 10.18632/oncotarget.2270 [PubMed: 25156567]
13. El-Naggar S, Liu Y, Dean DC. Mutation of the Rb1 pathway leads to overexpression of mTor, constitutive phosphorylation of Akt on serine 473, resistance to anoikis, and a block in c-Raf activation. Mol Cell Biol. 2009; 29(21):5710–7. DOI: 10.1128/MCB.00197-09 [PubMed: 19703998]
14. Nam HY, Han MW, Chang HW, Kim SY, Kim SW. Prolonged autophagy by MTOR inhibitor leads radioresistant cancer cells into senescence. Autophagy. 2013; 9(10):1631–2. DOI: 10.4161/auto.25879 [PubMed: 23989658]
15. Galanis E, Buckner JC, Maurer MJ, Kreisberg JI, Ballman K, Boni J, et al. Phase II trial of temsirolimus (CCI-779) in recurrent glioblastoma multiforme: a North Central Cancer Treatment Group Study. J Clin Oncol. 2005; 23(23):5294–304. DOI: 10.1200/JCO.2005.23.622 [PubMed: 15998902]
16. Li Z, Bao S, Wu Q, Wang H, Eyler C, Sathornsumetee S, et al. Hypoxia-inducible factors regulate tumorigenic capacity of glioma stem cells. Cancer Cell. 2009; 15(6):501–13. DOI: 10.1016/j.ccr.2009.03.018 [PubMed: 19477429]

17. Olmez I, Shen W, McDonald H, Ozpolat B. Dedifferentiation of patient-derived glioblastoma multiforme cell lines results in a cancer stem cell-like state with mitogen-independent growth. J Cell Mol Med. 2015; 19(6):1262–72. DOI: 10.1111/jcmm.12479 [PubMed: 25787115]

18. Chou TC. Drug combination studies and their synergy quantification using the Chou-Talalay method. Cancer Res. 2010; 70(2):440–6. DOI: 10.1158/0008-5472.CAN-09-1947 [PubMed: 20068163]

19. Fitzgerald JB, Schoeberl B, Nielsen UB, Sorger PK. Systems biology and combination therapy in the quest for clinical efficacy. Nat Chem Biol. 2006; 2(9):458–66. DOI: 10.1038/nchembio817 [PubMed: 16921358]

20. Hu W, Sung T, Jessen BA, Thibault S, Finkelstein MB, Khan NK, et al. Mechanistic Investigation of Bone Marrow Suppression Associated with Palbociclib and its Differentiation from Cytotoxic Chemotherapies. Clin Cancer Res. 2016; 22(8):2000–8. DOI: 10.1158/1078-0432.CCR-15-1421 [PubMed: 26631614]

21. Carracedo A, Ma L, Teruya-Feldstein J, Rojo F, Salmena L, Alimonti A, et al. Inhibition of mTORC1 leads to MAPK pathway activation through a PI3K-dependent feedback loop in human cancer. J Clin Invest. 2008; 118(9):3065–74. DOI: 10.1172/JCI34739 [PubMed: 18725988]

22. Mendoza MC, Er EE, Blenis J. The Ras-ERK and PI3K-mTOR pathways: cross-talk and compensation. Trends Biochem Sci. 2011; 36(6):320–8. DOI: 10.1016/j.tibs.2011.03.006 [PubMed: 21531565]

23. Sumi NJ, Kuenzi BM, Knezevic CE, Remsing Rix LL, Rix U. Chemoproteomics Reveals Novel Protein and Lipid Kinase Targets of Clinical CDK4/6 Inhibitors in Lung Cancer. ACS Chem Biol. 2015; 10(12):2680–6. DOI: 10.1021/acschembio.5b00368 [PubMed: 26390342]

24. Laplante M, Sabatini DM. mTOR signaling at a glance. J Cell Sci. 2009; 122(Pt 20):3589–94. DOI: 10.1242/jcs.051011 [PubMed: 19812304]

25. Vander Heiden MG, Cantley LC, Thompson CB. Understanding the Warburg effect: the metabolic requirements of cell proliferation. Science. 2009; 324(5930):1029–33. DOI: 10.1126/science.1160809 [PubMed: 19460998]

26. Minocha M, Khurana V, Qin B, Pal D, Mitra AK. Co-administration strategy to enhance brain accumulation of vandetanib by modulating P-glycoprotein (P-gp/Abcb1) and breast cancer resistance protein (Bcrp1/Abcg2) mediated efflux with m-TOR inhibitors. Int J Pharm. 2012; 434(1–2):306–14. DOI: 10.1016/j.ijpharm.2012.05.028 [PubMed: 22633931]

27. Mason WP. Blood-brain barrier-associated efflux transporters: a significant but underappreciated obstacle to drug development in glioblastoma. Neuro Oncol. 2015; 17(9):1181–2. DOI: 10.1093/neuonc/nov122 [PubMed: 26138634]

28. Parrish KE, Pokorny J, Mittapalli RK, Bakken K, Sarkaria JN, Elmquist WF. Efflux transporters at the blood-brain barrier limit delivery and efficacy of cyclin-dependent kinase 4/6 inhibitor palbociclib (PD-0332991) in an orthotopic brain tumor model. J Pharmacol Exp Ther. 2015; 355(2):264–71. DOI: 10.1124/jpet.115.228213 [PubMed: 26354993]

29. de Gooijer MC, Zhang P, Thota N, Mayayo-Peralta I, Buil LC, Beijnen JH, et al. P-glycoprotein and breast cancer resistance protein restrict the brain penetration of the CDK4/6 inhibitor palbociclib. Invest New Drugs. 2015; 33(5):1012–9. DOI: 10.1007/s10637-015-0266-y [PubMed: 26123925]

30. Sherr CJ, Beach D, Shapiro GI. Targeting CDK4 and CDK6: From Discovery to Therapy. Cancer Discov. 2016; 6(4):353–67. DOI: 10.1158/2159-8290.CD-15-0894 [PubMed: 26658964]

31. Johnson DB, Puzanov I. Treatment of NRAS-mutant melanoma. Curr Treat Options Oncol. 2015; 16(4):15.doi: 10.1007/s11864-015-0330-z [PubMed: 25796376]

32. Sosman JA, Kittaneh M, Lolkema MPJK, Postow MA, Schwartz G, Franklin C, et al. A phase 1b/2 study of LEE011 in combination with binimetinib (MEK162) in patients with NRAS -mutant melanoma: early encouraging clinical activity. J Clin Oncol. 2014; 32(suppl) abstr 9009.

33. Yao JC, Shah MH, Ito T, Bohas CL, Wolin EM, Van Cutsem E, et al. Everolimus for advanced pancreatic neuroendocrine tumors. N Engl J Med. 2011; 364(6):514–23. DOI: 10.1056/NEJMoa1009290 [PubMed: 21306238]

34. Yao JC, Fazio N, Singh S, Buzzoni R, Carnaghi C, Wolin E, et al. Everolimus for the treatment of advanced, non-functional neuroendocrine tumours of the lung or gastrointestinal tract

(RADIANT-4): a randomised, placebo-controlled, phase 3 study. Lancet. 2016; 387(10022):968–77. DOI: 10.1016/S0140-6736(15)00817-X [PubMed: 26703889]

35. Motzer RJ, Escudier B, Oudard S, Hutson TE, Porta C, Bracarda S, et al. Efficacy of everolimus in advanced renal cell carcinoma: a double-blind, randomised, placebo-controlled phase III trial. Lancet. 2008; 372(9637):449–56. DOI: 10.1016/S0140-6736(08)61039-9 [PubMed: 18653228]
36. Franz DN, Belousova E, Sparagana S, Bebin EM, Frost M, Kuperman R, et al. Efficacy and safety of everolimus for subependymal giant cell astrocytomas associated with tuberous sclerosis complex (EXIST-1): a multicentre, randomised, placebo-controlled phase 3 trial. Lancet. 2013; 381(9861):125–32. DOI: 10.1016/S0140-6736(12)61134-9 [PubMed: 23158522]
37. Mason WP, Macneil M, Kavan P, Easaw J, Macdonald D, Thiessen B, et al. A phase I study of temozolomide and everolimus (RAD001) in patients with newly diagnosed and progressive glioblastoma either receiving or not receiving enzyme-inducing anticonvulsants: an NCIC CTG study. Invest New Drugs. 2012; 30(6):2344–51. DOI: 10.1007/s10637-011-9775-5 [PubMed: 22160854]
38. Franco J, Balaji U, Freinkman E, Witkiewicz AK, Knudsen ES. Metabolic Reprogramming of Pancreatic Cancer Mediated by CDK4/6 Inhibition Elicits Unique Vulnerabilities. Cell Rep. 2016; 14(5):979–90. DOI: 10.1016/j.celrep.2015.12.094 [PubMed: 26804906]
39. Ku BM, Yi SY, Koh J, Bae YH, Sun JM, Lee SH, et al. The CDK4/6 inhibitor LY2835219 has potent activity in combination with mTOR inhibitor in head and neck squamous cell carcinoma. Oncotarget. 2016; 7(12):14803–13. DOI: 10.18632/oncotarget.7543 [PubMed: 26909611]
40. Subbiah V, Berry J, Roxas M, Guha-Thakurta N, Subbiah IM, Ali SM, et al. Systemic and CNS activity of the RET inhibitor vandetanib combined with the mTOR inhibitor everolimus in KIF5B-RET re-arranged non-small cell lung cancer with brain metastases. Lung Cancer. 2015; 89(1):76–9. DOI: 10.1016/j.lungcan.2015.04.004 [PubMed: 25982012]
41. Schwartz GK, LoRusso PM, Dickson MA, Randolph SS, Shaik MN, Wilner KD, et al. Phase I study of PD 0332991, a cyclin-dependent kinase inhibitor, administered in 3-week cycles (Schedule 2/1). Br J Cancer. 2011; 104(12):1862–8. DOI: 10.1038/bjc.2011.177 [PubMed: 21610706]
42. Flaherty KT, Lorusso PM, Demichele A, Abramson VG, Courtney R, Randolph SS, et al. Phase I, dose-escalation trial of the oral cyclin-dependent kinase 4/6 inhibitor PD 0332991, administered using a 21-day schedule in patients with advanced cancer. Clin Cancer Res. 2012; 18(2):568–76. DOI: 10.1158/1078-0432.CCR-11-0509 [PubMed: 22090362]
43. Jones NP, Schulze A. Targeting cancer metabolism--aiming at a tumour's sweet-spot. Drug Discov Today. 2012; 17(5–6):232–41. DOI: 10.1016/j.drudis.2011.12.017 [PubMed: 22207221]
44. Vander Heiden MG. Targeting cancer metabolism: a therapeutic window opens. Nat Rev Drug Discov. 2011; 10(9):671–84. DOI: 10.1038/nrd3504 [PubMed: 21878982]
45. Clem BF, Chesney J. Molecular pathways: regulation of metabolism by RB. Clin Cancer Res. 2012; 18(22):6096–100. DOI: 10.1158/1078-0432.CCR-11-3164 [PubMed: 23154086]
46. Lopez-Mejia IC, Fajas L. Cell cycle regulation of mitochondrial function. Curr Opin Cell Biol. 2015; 33:19–25. DOI: 10.1016/j.ceb.2014.10.006 [PubMed: 25463842]
47. Escote X, Fajas L. Metabolic adaptation to cancer growth: from the cell to the organism. Cancer Lett. 2015; 356(2 Pt A):171–5. DOI: 10.1016/j.canlet.2014.03.034 [PubMed: 24709629]

Statement of Translational Relevance

Glioblastoma is the most common aggressive brain tumor, taking over 10,000 lives each year in the U.S. alone. It has proven relatively resistant both to standard therapies and to newer targeted therapies. Inhibitors of the mTOR and CDK/RB pathways have both been shown to have activity in certain cancers, but have proven disappointing in trials for glioblastoma. We show for the first time that combining mTOR and CDK4/6 inhibition has synergistic effects against glioblastoma stem cell lines *in vitro* and *in vivo*. This synergy appears to act through multiple mechanisms, including cross-regulation by each inhibitor of the other pathway, convergence on Erk signaling, and an mTOR inhibitor-driven increase in brain levels of the CDK4/6 inhibitor. These results have direct therapeutic implications, suggesting the need for testing this combination in a clinical trial.

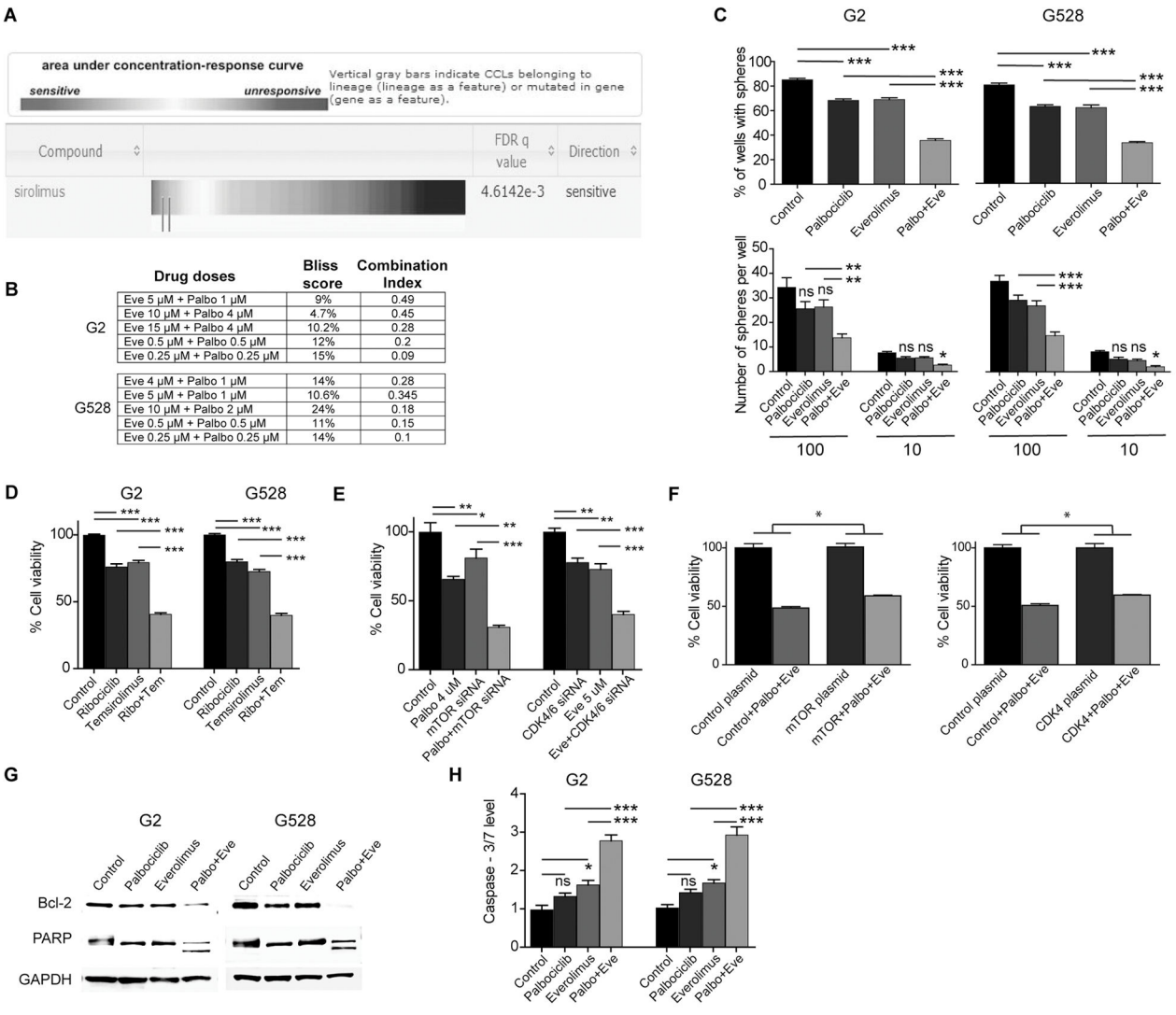

Figure 1. The combination of CDK4/6 and mTOR inhibition is synergistic against GBM

(**A**) Enrichment analysis showing increased sensitivity of cancer lines with mutations in *RB1* to an mTOR inhibitor, sirolimus. (**B**) Synergy scores of the combination of CDK4/6 and mTOR inhibition in two GIC lines calculated with both the Bliss and the Chou-Talalay methods. (**C**) 10 and 100 GICs were cultured in 24-well plates over two weeks to compare sphere formation upon treatment with vehicle, palbociclib (1 μM), everolimus (4 μM), and the combination of palbociclib and everolimus (*$P < 0.05$; **$P < 0.001$; ***$P < 0.0001$; one-way analysis of variance (ANOVA) with post-hoc Tukey analysis). (**D**) The combination of a different mTOR inhibitor temsirolimus (4 μM) and a different CDK4/6 inhibitor ribociclib (4 μM) is also synergistic against GICs (***$P < 0.0001$; one-way ANOVA with post-hoc Tukey analysis). (**E**) The combinations of palbociclib (4 μM) with mTOR siRNA and everolimus (5 μM) with CDK4/6 siRNA are also synergistic against GICs (each treatment line received either DMSO or the indicated drug and either control siRNA or a specific siRNA) (**$P < 0.001$; ***$P < 0.0001$; one-way ANOVA with post-hoc Tukey analysis). (**F**) Constitutively-active CDK4 and mTOR plasmids partially rescued from the effects of the

combination treatment (each treatment line received either a control plasmid or the indicated active plasmid and either DMSO or the combination treatment) (*$P < 0.05$; two-tailed *t*-test). (**G** and **H**) Combined CDK4/6 and mTOR inhibition induces significant apoptosis. Shown is an immunoblot using antibodies specific for Bcl-2 and PARP. Caspase-3/7 level is increased with the three days of combined treatment. (*$P < 0.05$; ***$P < 0.0001$; one-way ANOVA with post-hoc Tukey analysis).

Eve: Everolimus, Palbo: Palbociclib, Ribo: Ribociclib, Tem: Temsirolimus, NS: Non-Significant. All values are mean ± SEM of triplicates. Cell viabilities were determined via cell counts following 3 days of treatment. Each experiment was performed 3 times using separate samples.

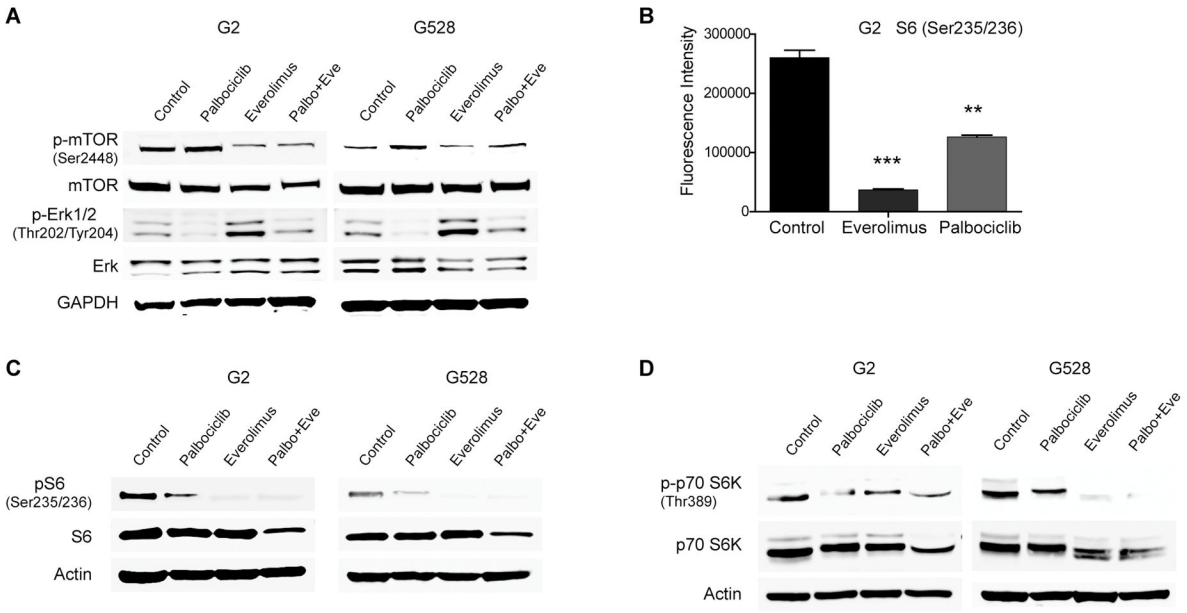

Figure 2. CDK4/6 inhibition and mTOR inhibition cooperate through multiple pathways

(**A**) Palbociclib and everolimus have contrasting effects on mTOR and Erk activities. Shown is an immunoblot using antibodies specific for mTOR and Erk. (**B**–**C**) Palbociclib treatment decreases the phosphorylation of S6. Shown is an antibody array (ELISA) and an immunoblot using antibodies specific for S6 (** $P < 0.001$; *** $P < 0.0001$; one-way ANOVA with post-hoc Tukey analysis. Values are mean ± SEM of triplicates). (**D**) The phosphorylation of p70S6K is decreased with palbociclib treatment. Shown is an immunoblot using antibodies specific for p70S6K.

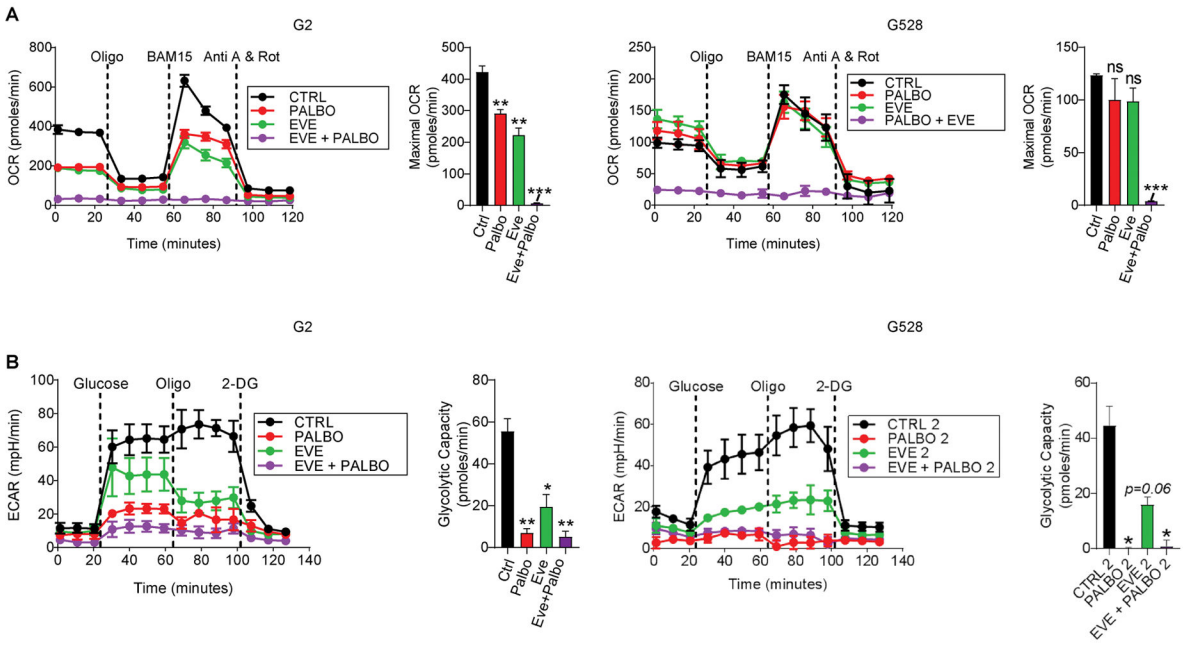

Figure 3. Combined CDK4/6 and mTOR inhibition disrupts GIC metabolism

(**A**) Oxygen consumption rate (OCR) and the maximal OCR were measured using a Seahorse XF 24 Flux Analyzer in two GIC lines made adherent as per Methods and subjected to a mitochondrial stress test. (**B**) Extracellular acidification rate (ECAR) and the glycolytic capacity were measured in two GIC lines subjected to a glycolytic stress test (*$P < 0.05$; **$P < 0.001$; ***$P < 0.0001$; one-way ANOVA with post-hoc Tukey analysis. Values are mean ± SEM of triplicates). Doses for palbociclib and everolimus were 1 μM and 2 μM, respectively.

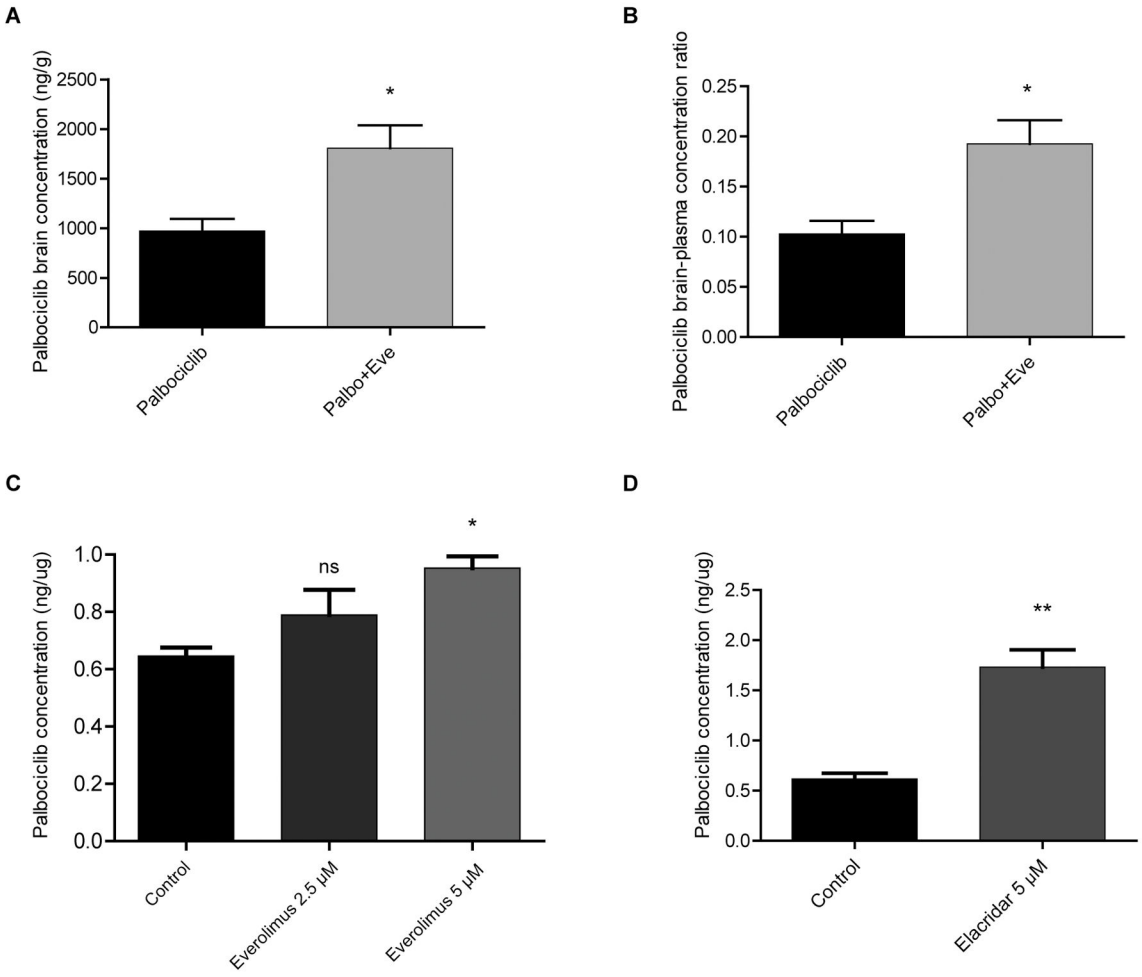

Figure 4. Everolimus significantly increases brain concentration of palbociclib

(**A**) Brain concentration and (**B**) brain-to-plasma concentration ratio of palbociclib either alone or in the presence of everolimus following three days of once-daily oral treatment in wild type mice (n =4; values are mean ± SEM. *P < 0.05; two-tailed t-test). (**C–D**) Everolimus co-administration drives a moderate increase in intracellular palbociclib concentration in human brain microvascular endothelial cells, as does the very potent P-gp and BCRP inhibitor elacridar (*P = 0.01; **P < 0.003; two-tailed t-test).

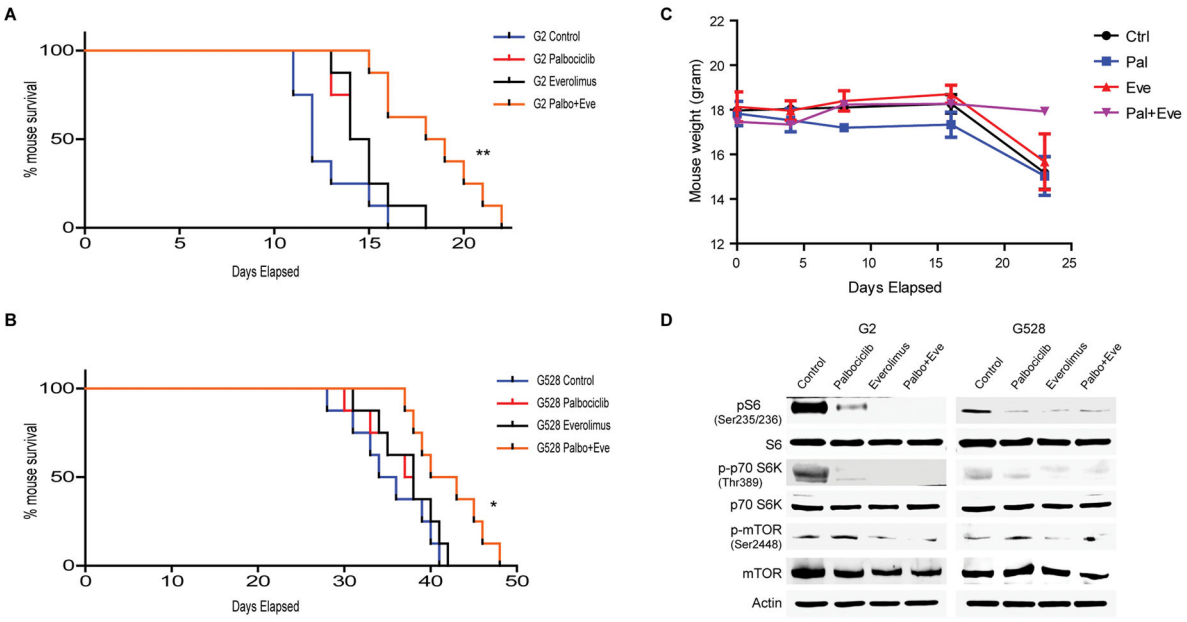

Figure 5. ***In vivo*** **efficacy of combined CDK4/6 and mTOR inhibition**

(**A**–**B**) Kaplan-Meier survival curves of mouse xenografts with two different GIC lines treated with palbociclib (50 mg/kg via oral gavage, four days a week), everolimus (5 mg/kg via oral gavage, four days a week), and the combination of both showing significantly prolonged survival with the combined treatment (*$P < 0.05$; **$P < 0.001$, $n = 8$ mice per cohort). (**C**) Mouse body weight comparison of each treatment group. (**D**) Both palbociclib and everolimus modify their targets *in vivo* as well. Shown is an immunoblot using antibodies specific for mTOR, S6, and p70S6K.

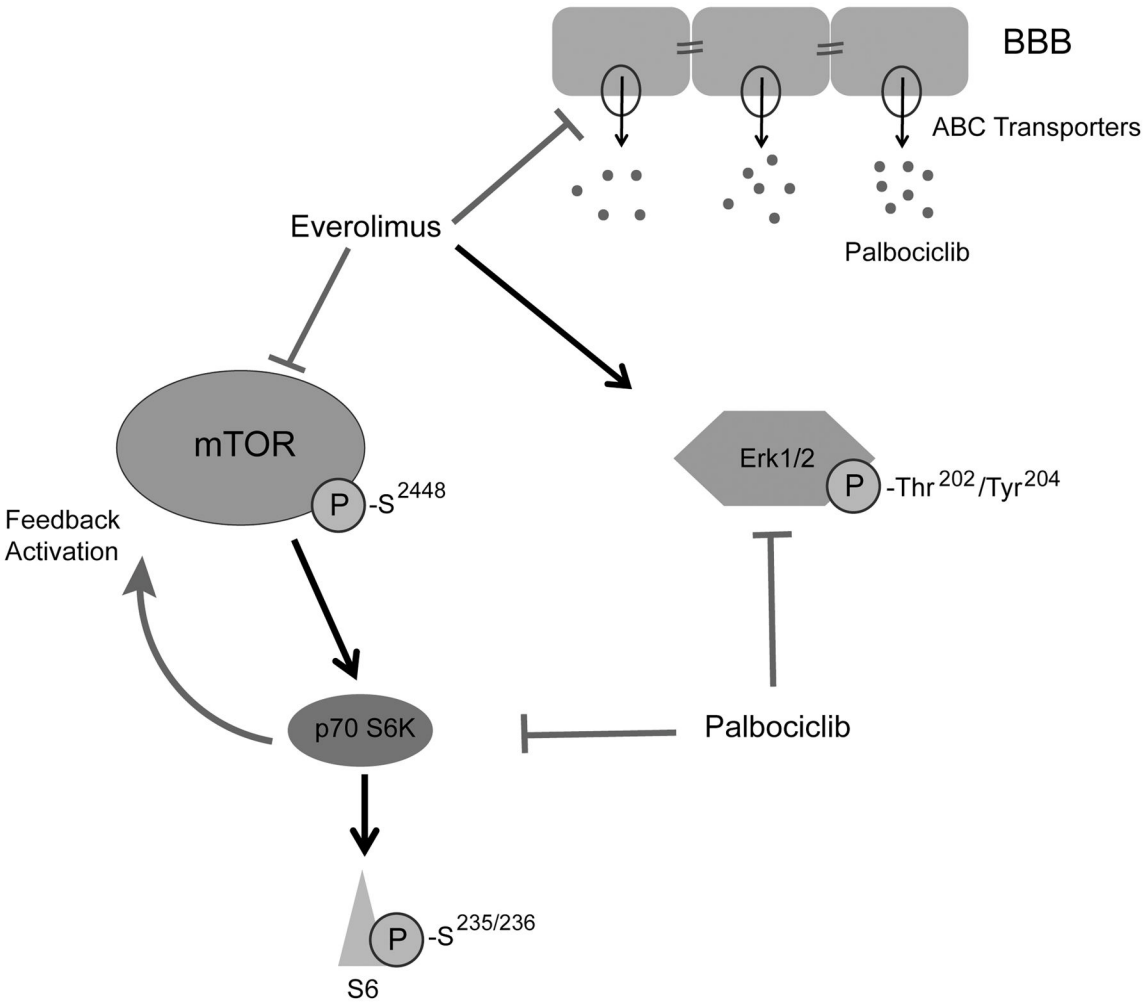

Figure 6. Schematic depicting the cooperation between everolimus and palbociclib